 Human Molecular Genetics, 2002, Vol. 11, No. 8 971–979

Mutations in *TITF-1* are associated with benign hereditary chorea

Guido J. Breedveld[1], Jeroen W.F. van Dongen[1], Cesare Danesino[2], Andrea Guala[3], Alan K. Percy[4], Leon S. Dure[4], Peter Harper[5], Lazarus P. Lazarou[5], Herma van der Linde[1], Marijke Joosse[1], Annette Grüters[6], Marcy E. MacDonald[7], Bert B.A. de Vries[8], Willem Frans M. Arts[9], Ben A. Oostra[1], Heiko Krude[7] and Peter Heutink[1,*]

[1]Department of Clinical Genetics, Erasmus University, Rotterdam, The Netherlands, [2]Department of Medical Genetics, University of Pavia, Italy, [3]Pediatric UAO, ASL 11, Hospital SS Pietro e Paolo, Borgosesesia, Italy, [4]Division of Pediatric Neurology, University of Alabama at Birmingham, USA, [5]Department of Medicine, University of Wales, Cardiff, UK, [6]Otto-Heubner-Centrum for Pediatrics, Charite, Humbold University, Berlin, Germany, [7]Molecular Neurogenetics Unit, Massachusetts General Hospital, Charlestown, USA, [8]Department of Human Genetics, University Medical Center Nijmegen, The Netherlands, [9]Department of Pediatric Neurology, Erasmus University Medical Center, Rotterdam, The Netherlands

Received January 23, 2002; Revised and Accepted February 19, 2002

DDBJ/EMBL/GenBank accession nos 104378–104380, G73507–G73510

Benign hereditary chorea (BHC) (MIM 118700) is an autosomal dominant movement disorder. The early onset of symptoms (usually before the age of 5 years) and the observation that in some BHC families the symptoms tend to decrease in adulthood suggests that the disorder results from a developmental disturbance of the brain. In contrast to Huntington disease (MIM 143100), BHC is non-progressive and patients have normal or slightly below normal intelligence. There is considerable inter- and intrafamilial variability, including dysarthria, axial dystonia and gait disturbances. Previously, we identified a locus for BHC on chromosome 14 and subsequently identified additional independent families linked to the same locus. Recombination analysis of all chromosome 14-linked families resulted initially in a reduction of the critical interval for the BHC gene to 8.4 cM between markers D14S49 and D14S278. More detailed analysis of the critical region in a small BHC family revealed a *de novo* deletion of 1.2 Mb harboring the *TITF-1* gene, a homeodomain-containing transcription factor essential for the organogenesis of the lung, thyroid and the basal ganglia. Here we report evidence that mutations in *TITF-1* are associated with BHC.

INTRODUCTION

Benign hereditary chorea (BHC) (MIM 118700) is an autosomal dominant movement disorder. The disorder manifests itself before the age of 5 years, running a stationary or only slightly progressive course (1,2). The intelligence is normal or slightly below normal, and mental deterioration as found in Huntington disease (HD) (3,4) is not seen. In some families, the choreic movements tend to decrease during adolescence or early adulthood (5). The early onset of symptoms and the observation that symptoms tend to decrease in adulthood suggest that the disorder results from a developmental disturbance of the brain.

Since the first BHC report in 1966 (6), a large number of families have been reported (7). These families show considerable intra- and interfamilial phenotypic variation. Some exhibit additional atypical features such as axial or extremity dystonia, myoclonic jerks, dysarthria and gait disturbances (8). In many families, another diagnosis — such as HD, ataxia telangiectasia or benign essential myoclonus — was made during follow-up (9–11), leading some authors to doubt the existence of BHC as a separate disorder (12).

Previously, we identified a locus for BHC on chromosome 14 (13), and this finding was confirmed in an independent family (14). Since our original report, we have identified additional independent families linked to the same locus, as well as BHC families that provided evidence for non-linkage to chromosome 14, demonstrating that BHC is a genetically heterogeneous disorder (G.J. Breedveld et al., in preparation). Recombination analysis of the chromosome 14-linked families resulted initially

*To whom correspondence should be addressed at: Department of Clinical Genetics, Erasmus Medical Center Rotterdam, PO Box 1738, 3000 DR Rotterdam, The Netherlands. Tel: + 31 104088136; Fax: + 31 104089489; Email: heutink@kgen.fgg.eur.n

in a reduction of the critical interval for the BHC gene to 8.4 cM between markers D14S49 and D14S278 (G.J. Breedveld et al., in preparation). More detailed analysis of the critical region in a small BHC family revealed a de novo deletion of 1.2 Mb. Several genes were identified in this region, including the thyroid transcription factor 1 gene (TITF-1), also known as NKX2.1, T/EBP and TTF-1, of the NK2 family of homeodomain-containing transcription factors (15–18). Although most studies of TITF-1 have focussed on its role in thyroid and lung development, evidence from TITF-1 knockout mice demonstrates that the gene is essential for the differentiation of the striatum and the developing brain (19–22). Given its function, TITF-1 is therefore an excellent candidate gene for BHC. Here we report evidence that mutations in TITF-1 are associated with BHC.

RESULTS

Four independent BHC families were studied. Linkage to chromosome 14 has been previously described for Dutch family 1 (NL1) (13), and a large family from the USA (US1) (23) (G.J. Breedveld et al., in preparation). In an Italian family (IT1) (24) and a family from the UK (UK1) (5), linkage to chromosome 14 could be neither confirmed nor excluded because of the limited numbers of samples available for testing.

Analysis of markers from chromosome 14 in family IT1 revealed a lack of transmission of the maternal allele for the short tandem repeat (STR) marker D14S1017 from individual II-4 to III-1 (Fig. 1). To exclude a polymorphism within a primer sequence, or other technical reasons for the failure of the amplification of this allele, new primers were designed for this marker and tested. We confirmed the lack of transmission of the maternal allele, suggesting that a de novo deletion within the maternal chromosome had occurred (Fig. 1). To define the exact borders of this deletion, we developed several new polymorphic STR markers, on the basis of known genomic sequence, within the region and tested them on the family. The proximal boundary of the deletion could be pinpointed between markers CGR67 and CGR46, whereas the distal boundary was placed between CGR58 and CGR69, a region spanning about 1.2 Mb on the genomic level (Fig. 2). Subsequently, the deletion was confirmed by two-color FISH hybridization (Fig. 3) using two bacterial artificial chromosome (BAC) clones

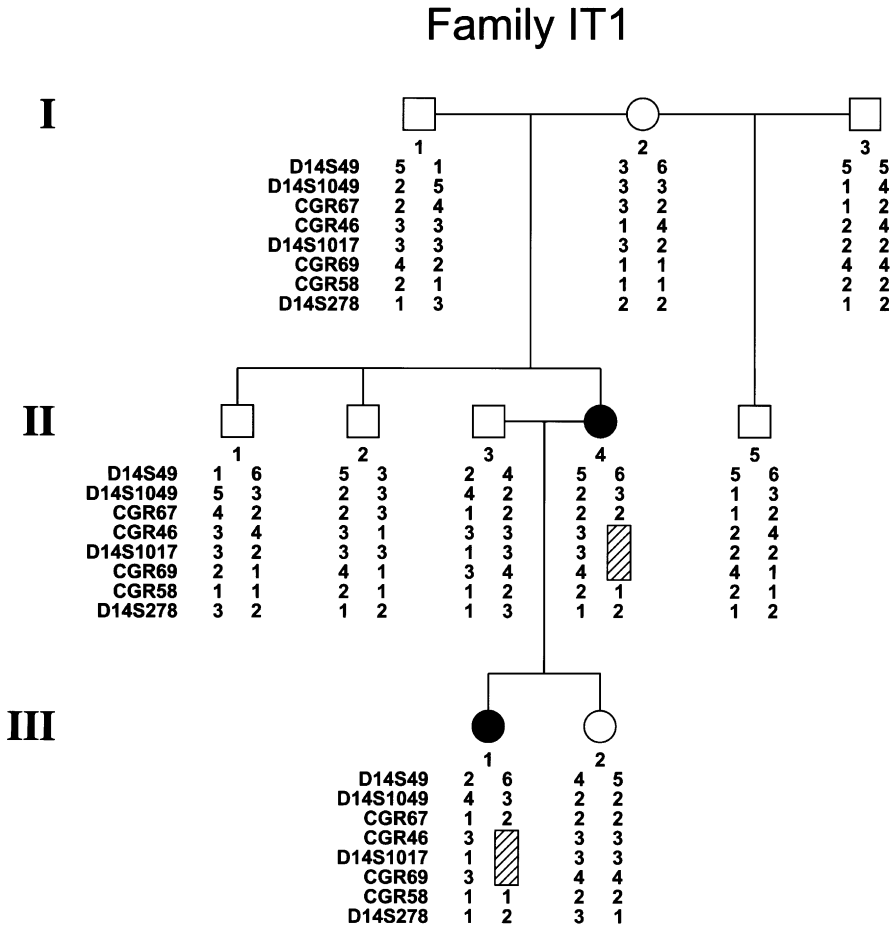

Figure 1. Haplotype reconstruction of eight chromosome 14q13.1 STR markers in family IT1, showing that a de novo deletion within a grandmaternal allele (individual I-2) is inherited by individuals II-4 and III-1. Black symbols represent BHC-affected individuals, open symbols represent unaffected individuals. The hatched boxes indicate the minimum deletion region defined by hemizygosity of marker CGR46 in person II-4 and marker CGR69 in person III-1. The maximum deletion region is defined owing to heterozygosity of marker CGR58 in person II-4 and marker CGR67 in person III-1.

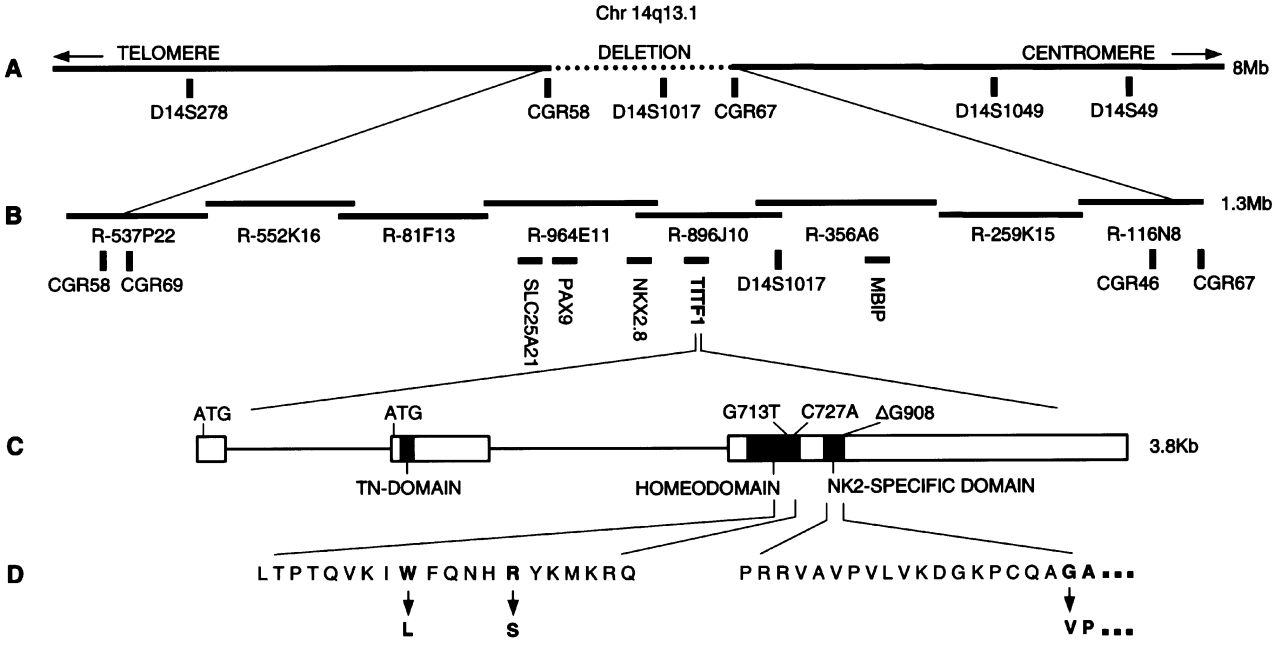

Figure 2. Genomic organization of the TITF-1 gene. (A) An 8 Mb region of chromosome 14q13.1 is shown with the deletion interval found in family IT1 and STR markers. (B) Overlapping BAC contig; STR markers and annotated genes of the 1.2 Mb deletion interval. (C) Genomic organization of the TITF-1 gene, consisting of three exons spanning 3.8 kb; ATGs indicate both start codons of the ORF; conserved domains are indicated by black boxes. TITF-1 mutations found in families US1 (G713T), NL1 (C727A) and UK1 (ΔG908) are indicated. (D) Partial amino acid sequence surrounding identified mutations and predicted amino acid changes (in bold) resulting from the G713T, C727A and ΔG908 mutations, respectively.

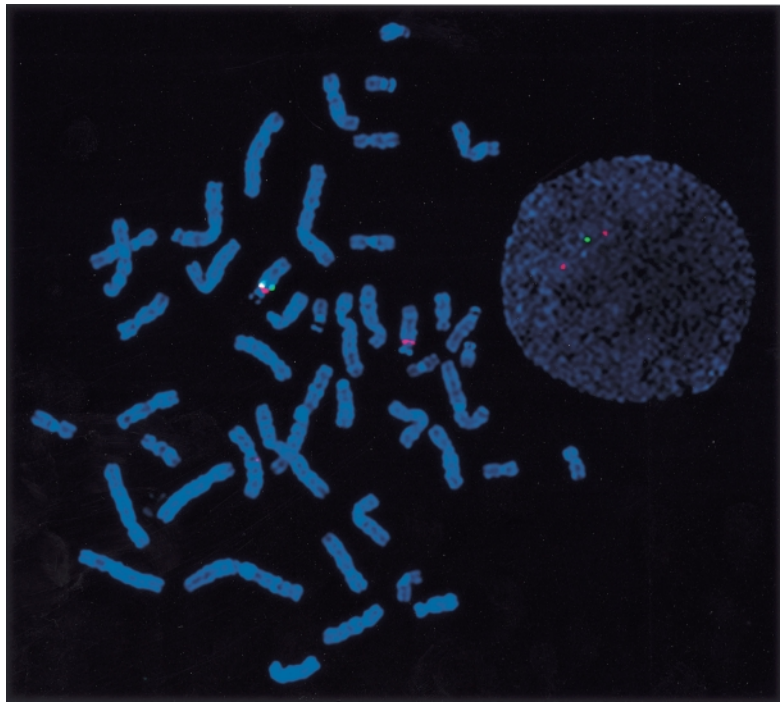

Figure 3. Two-color FISH analysis using chromosome 14q11 BAC 2577N12 (red signal) and chromosome 14q13.1 BAC 552K16 (green signal) on metaphase and interphase chromosomes derived from a culture of EBV-transformed lymphocytes of BHC patient III-1 in family IT1. Both chromosome 14 homologues display a red signal, whereas only one chromosome 14 showed a green signal indicating a genomic deletion of BAC 552K16 sequences.

as probes. BAC clone RP11-552K16 lies within the apparent genomic deletion, between markers CGR69 and D14S1017 (Fig. 2). BAC clone C-2577N12 is located outside the apparent deletion, in the proximity of D14S49 (Fig. 2). With BAC C-2577N12, both copies of chromosome 14 were detected on a chromosomal spread from Epstein–Barr Virus (EBV)-transformed lymphocytes from patient III-1 of family IT1. BAC R-552K16, in contrast, showed only one signal for chromosome 14; no signal was detected on any of the other chromosomes, confirming that indeed there is a genomic deletion segregating in this family. Since individuals I-1 and I-2 showed heterozygosity for several markers within the deletion and had no family history of chorea, the most likely explanation is that a de novo mutation in an oocyte of individual I-2 was transmitted to individual II-3 and subsequently to individual III-1. The deletion was not seen in two other unaffected subjects in this family who inherited the maternal chromosome without the deletion. No deletions were detected in families NL1 and US1 using the same STR markers as above within the 1.2 Mb region.

A transcript map was constructed using sequence information from available genome databases, and we searched for expressed sequences within the 1.2 Mb deleted region. Five transcripts were identified, encoding the following genes: thyroid transcription factor 1 (TITF-1), MAPK upstream kinase (MUK)-binding inhibitory protein (MBIP), NK-2 Drosophila homologue 8 (NKX2.8), paired box gene 9 (PAX9) and solute carrier family 25 member 21 (SLC25A21) (Fig. 2).

TITF-1 encompasses three exons spanning a genomic region of 3.8 kb (25). Two major transcripts are produced, of 2.3 and 2.5 kb, encoding proteins of 371 and 401 amino acids, respectively (26). The two protein isoforms differ only at their N termini. The functional significance of these two protein isoforms is unknown. After determining the intron–exon boundaries of the TITF-1 gene, using available sequence databases, the coding region including intron–exon boundaries was sequenced on genomic DNA in patients from BHC families NL1, US1 and UK1.

In family NL1, we detected a heterozygous C-to-A transversion at position 727 (C727A) from the coding region (Fig. 4) (reference sequence XM_048680), resulting in an amino acid substitution of arginine by serine at codon 243 (R243S). The mutation segregated with the disease in all available diagnosed family members of family NL1 (Fig. 5). The mutation was not seen in 200 control chromosomes from the general population. From three subjects with an uncertain diagnosis (13), individuals II-14 and III-13 inherited the mutation whereas the mutation was absent in individual IV-4, demonstrating the problems with clinical diagnosis of BHC; individual II-14 was diagnosed in childhood with Sydenham's chorea but this diagnosis had been revised, in our original study, to BHC. Subject III-13 did not show abnormalities at physical examination at age 29 years, and has an unclear history of choreic movements. Individual IV-4 had ataxic diplegia and no obvious signs of chorea, but was only 3 years old at time of the clinical investigation.

Family US1 showed a heterozygous G-to-T base change at position 713 (G713T) (Fig. 4), resulting in a substitution of tryptophan by leucine at codon 238 (W238L). The mutation was seen in all available affected pedigree members but not in unaffected family members (Fig. 5) or in 200 control chromosomes from the general population.

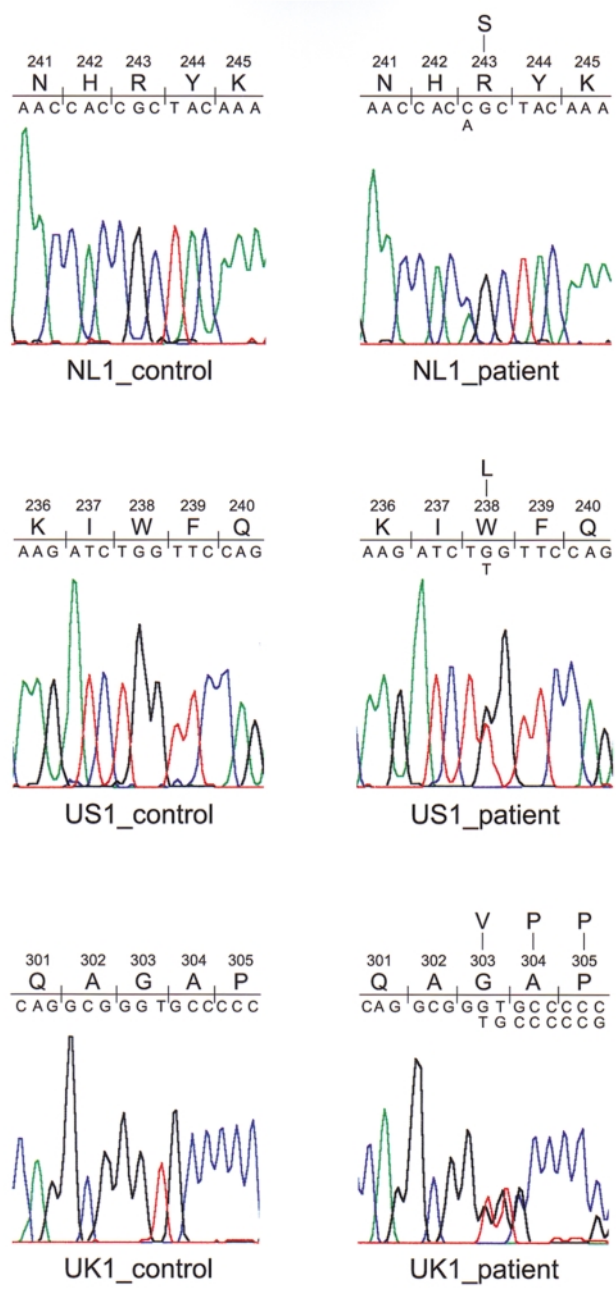

Figure 4. Sequence electropherograms of mutations found in TITF-1. Both normal (left) and mutated (right) DNA and amino acid sequences are shown. From top to bottom: the heterozygous C-to-A transversion at position 727 (C727A) resulting in an amino acid substitution of arginine by serine at codon 243 (R243S) in family NL1; the heterozygous G-to-T base change at position 713 (G713T) resulting in a substitution of tryptophan by leucine at codon 238 (W238L) in family US1; the heterozygous deletion of a G at position 908 (ΔG908), resulting in a frameshift of the reading frame in family UK1 (G303fsX77).

Finally, a patient from family UK1 showed a heterozygous deletion of a G at position 908 (ΔG908) (Fig. 4), resulting in a frameshift of the reading frame (G303fsX77). This frameshift

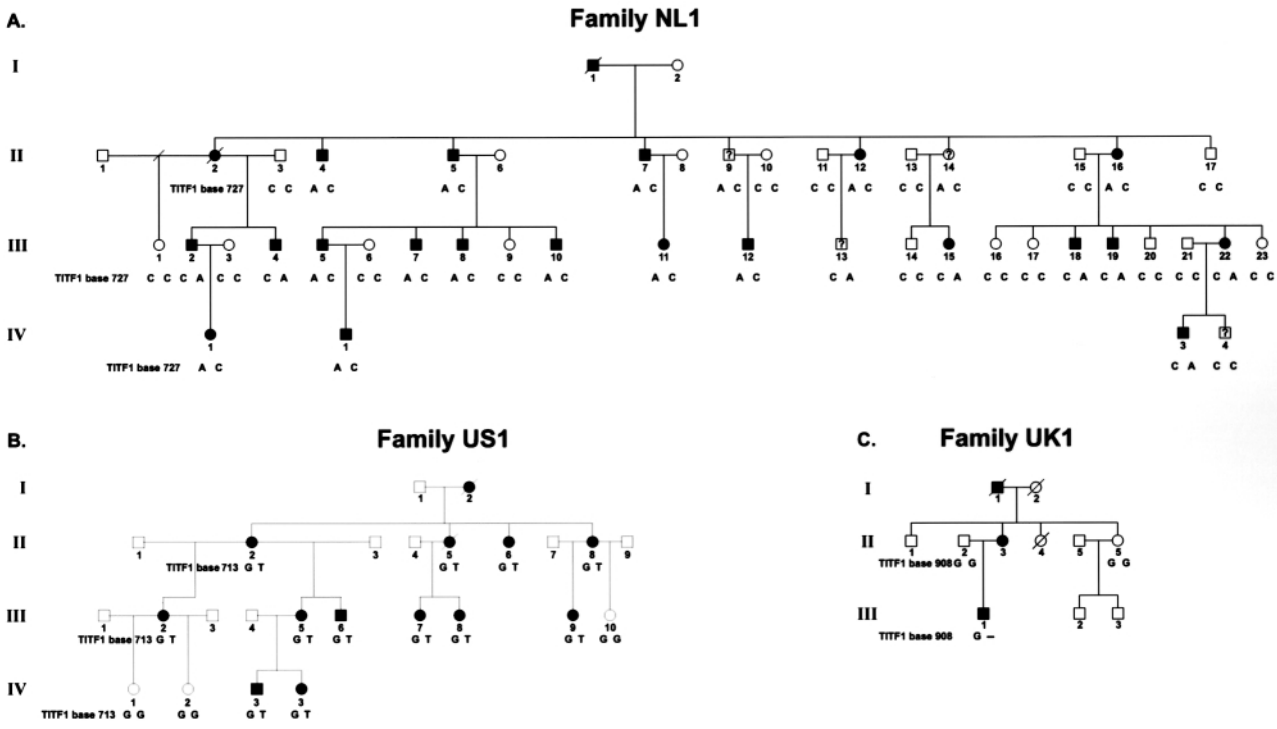

Figure 5. Segregation analysis of TITF-1 mutations found in families NL1 (C727A), US1 (G713T) and UK1 (G303fsX77). Black symbols represent BHC-affected individuals, open symbols represent unaffected individuals and a question mark within a symbol denotes diagnosis unknown (II-9) or uncertain (II-14, III-13, IV-4). For each mutation, both the normal and mutated nucleotides are indicated. The deleted nucleotide in UK 1 is indicated by a dash.

results in an aberrant protein starting at codon 303 extending 77 amino acids followed by a premature stop at codon 380 (22 amino acids missing). This mutation could not be detected in two unaffected individuals of the family (Fig. 5) or in 200 control chromosomes from the general population. The mutations were not seen in publicly available single nucleotide polymorphism (SNP) and sequence databases or the Celera human genome SNP database.

DISCUSSION

BHC is an autosomal dominant neurological disorder. At least two loci exist, one on chromosome 14q and one unknown locus (G.J. Breedveld et al., in preparation). We have identified mutations in the TITF-1 gene on chromosome 14. The R243S and W238L mutations in families NL1 and US1 are affecting highly conserved amino acids in the homeodomain of the TITF-1 gene (Fig. 6) (18). Homeodomains are DNA-binding domains with a helix–turn–helix motif. The mutations are located in helix 3, which upon binding to genomic DNA is positioned within the wide groove of DNA and is responsible for the majority of contacts between the target DNA sequence and the TITF-1 protein (18,27,28).

The R243S mutation results in the change of a basic to a neutral residue in this region and is directly adjacent to the tyrosine residue (Y244) that is unique for the NKX class of homeodomain proteins and determines the specificity of binding to the DNA consensus sequence 5′ T(C/T)AAGTG 3′ (18,28). The W238L mutation is located at a hydrophobic position of the third helix, which is important for the proper positioning of the three helix subunits relative to each other (28). Both mutations are close to the glutamine (Q240) and asparagine (N241) residues, which are critical for base pair contacts, and are therefore expected to affect the DNA-binding properties of TITF-1 (18,27,28).

In contrast to the other mutations, ΔG908 is located within the NK2-specific domain (NK2-SD). The function of this domain is not known (18). The region is highly conserved in NK2 genes and is proline-rich. It contains a hydrophobic core with four valine residues in every second position and a flanking basic protein : protein interface. In vitro, this domain is not required for high-affinity sequence-specific DNA binding (15,28), but it has been suggested that the region might dock with factors that modulate transcriptional activation by TITF-1 in vivo (18). The frameshift introduced by this single base deletion also causes an aberrant C-terminus of the protein. The function of the C terminus of TITF-1 is unknown.

The genomic deletion in IT1 results in the complete loss of one TITF-1 allele, suggesting that the chorea phenotype in this family is caused by haploinsufficiency of the TITF-1 protein. The mutations within conserved amino acids of the homeobox DNA-binding domain of the transcription factor BHC most likely result in a loss of DNA binding of TITF-1 and thus in the loss of function of one TITF-1 allele.

In HD, signaling from the putamen to the external segment of the globus pallidus through the so-called indirect pathway is impaired owing to the loss of a subset of medium spiny neurons as a result of an expanded polyglutamine stretch in the huntingtin protein (29,30). The external segment of the globus

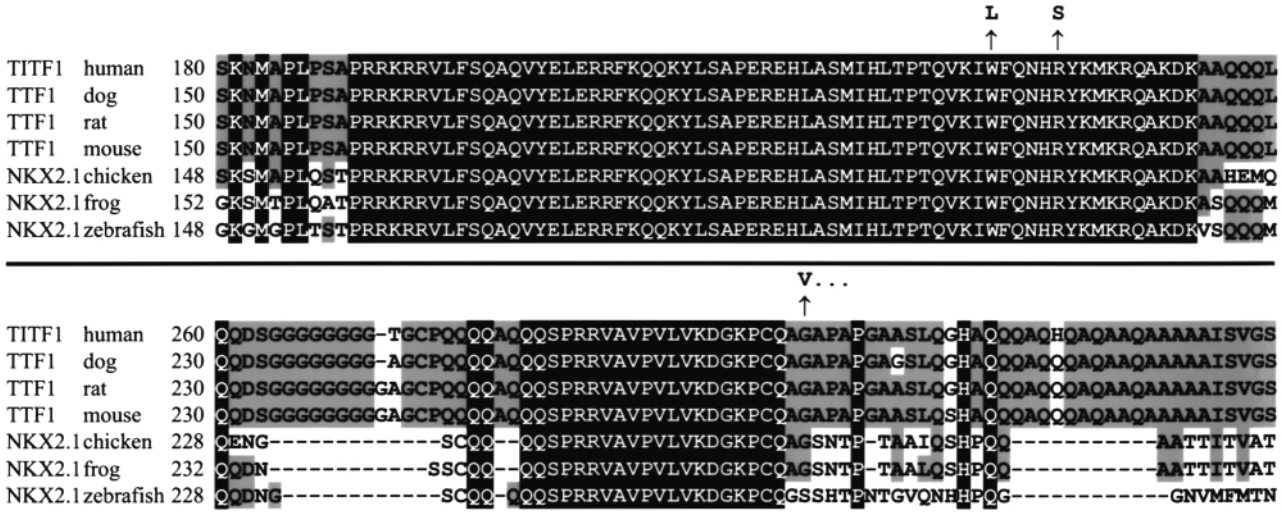

Figure 6. Alignment of the homeodomain and NK2-SD domain of the human TITF-1 protein with orthologs of other species (amino acids 180–338 form human TITF-1). Completely or partly conserved amino acids are represented on a black or gray background respectively; arrows indicate the positions of the mutations found in BHC family US1 (W238L), family NL1 (R243S) and family UK1 (G303fsX77). GenBank accession numbers: TTF1 dog: P43698; TTF1 rat: P23441; TTF1 mouse: NM_009385.1; NKX2.1 chicken: AJ223618.1; NKX2.1 frog: AF250347.1; NKX2.1 zebrafish: AF321112.1.

pallidus is essential for limiting stimulation of neurons to the thalamus. This alteration of basal ganglia activity results in a greater degree of inhibition of thalamic outflow to the cortex. Accepted models of basal ganglia function predict that loss of this inhibition leads to hyperkinesia and choreic movements. Hyperkinesia can also be expected when the ventral striatum (pallidum) or neurons within the indirect pathway are not properly connected, as in TITF-1 knockout mice (19,21). Mice lacking TITF-1 expression die at birth and have severe lung, thyroid and pituitary defects (19,21). In addition, TITF-1 is essential for the development of the basal ganglia. In TITF-1-deficient mice, the anlage from the ventral region of the striatum is transformed into more dorsal structures and the pallidum is not formed. TITF-1 is also required for the production of basal forebrain TrkA-positive neurons and the migration of GABAergic neurons to the cerebral cortex (21,22).

BHC is, however, an autosomal dominant disease with a loss of function of only one allele encoding the TITF-1 protein; the other allele is still fully functional. Furthermore, hemizygous TITF-1 mice develop normally, although neurological abnormalities have not been studied in detail (19,21). In patients, no abnormalities were detected on the available cranial MRI studies. When these patients reach adulthood, neurological symptoms usually become less severe or even disappear. It is therefore likely that the disturbance in development of patients is not as severe as in mice completely lacking TITF-1 expression. Instead, the reduction of functional TITF-1 protein could result in a delayed development of the basal ganglia, delayed or reduced formation of basal forebrain TrkA-positive neurons, and/or migration of GABAergic neurons to the cerebral cortex, leading to a reduced inhibition of the thalamus. The observation that clinical involvement tends to decrease after reaching adolescence or early adulthood suggests either that the brain compensates for the defect by re-routing neuronal signaling or that the role of TITF-1 with respect to the level of thyroid activity is important during neuronal growth and development, but is less critical during adult life. Resolution of this aspect remains to be determined by future study.

Heterozygous deletions of chromosome 14q including TITF-1 in humans are sometimes associated with thyroid dysfunction, lung distress, midline defects, brain abnormalities and movement disorders (31–35), but heterozygous TITF-1 mice do not show these abnormalities (21). In none of the families described here were lung and/or thyroid problems common, but thyroid function has not been systematically investigated. In family US1, at least one member was diagnosed with congenital hypothyroidism. In the families described here, only the TITF-1 gene is affected or, as in family IT1, five transcripts are deleted. A possible explanation would be that in all previously described cases of TITF-1 deletions, the deletions are much larger than found in our IT1 family and that there is a correlation between the phenotype severity and the size of the deletion intervals because other genes are deleted that also contribute to the phenotype. Alternatively, environmental factors or genetic background could influence the phenotype. Given the nature and diversity of the identified mutations affecting TITF-1, it will be of interest to extend the available clinical data of patients to include thyroid dysfunction, lung distress, midline defects and structural brain abnormalities in order to generate a genotype–phenotype correlation.

Several families with incomplete penetrance for BHC have been reported (8,36,37). The finding of a de novo deletion in one of our families might offer an alternative explanation. The reported segregation pattern might in fact be explained by de novo deletions instead of incomplete penetrance.

The observation of four different mutations provides strong evidence that mutations in TITF-1 are directly responsible for BHC in the families reported here. Several families with early-onset chorea are not linked to chromosome 14. Genes that

function within the TITF-1 pathway are now candidate genes for the disorder in these families, and the specificity of target DNA sequence of TITF-1 might help us to identify those genes.

In movement disorders such as Parkinson disease, tremors, dystonias and HD, the basal ganglia play an important role. The identification of mutations in TITF-1 resulting in BHC now prompts studies targeted towards a better understanding of the function of TITF-1 in the formation and function of the basal ganglia. The current findings also allow us to differentiate BHC from other movement disorders such as HD, ataxia telangiectasia and benign essential myoclonus.

MATERIALS AND METHODS

Clinical studies

Clinical symptoms of families have been described elsewhere (5,13,23,24). Medical ethical committees in all participating research institutes approved this study.

FISH studies

FISH studies were performed on metaphases and interphases derived from EBV-transformed peripheral blood lymphocytes of BHC patient III-1 of family IT1. A two-color FISH with a combination of a biotin-labeled probe (red) BAC C-2577N12 and a digoxigenin-labeled probe (green) BAC R-552K16 was done using standard protocols with minor modifications. Chromosomes were counterstained with 4,6-diamidino-2-phenylindole (DAPI) (blue). Slides were examined under a Leica Aristoplan fluorescence microscope and images were captured using a Genetiscan Power Gene System (PSI Ltd, Chester, UK).

STR marker development

Sequence data from BAC clones were downloaded from GenBank (http://www.ncbi.nlm.nih.gov/Genbank/index.html). STR sequences were selected by repeat length and type using the program FileProcessor (J.W. van Dongen, 2001) available at http://www.eur.nl/fgg/kgen. For databases and sequence analysis, see http://www.eur.nl/fgg/kgen (choose 'www links: Databases and Sequence Analysis').

Flanking primers were designed using Primer3 (http://www-genome.wi.mit.edu/genome_software/other/primer3.html).

Heterozygosity of markers was determined using a panel of 200 independent chromosomes from the general population. CGR46 and CGR67 were developed using the BAC R-116N8 sequence as source. CGR58 and CGR69 were developed from BAC R-537P22. D14S1017N was developed from R-896J10.

The following primer sequences were used to amplify these STRs:
D14S1017N; forward; tgttcttaccaaacaagcaaaca; reverse; ggacaaatgcatacacctgtga; size 146 bp.
CGR46; forward; ctgagcaagacaccgtcaga; reverse; cccaacaaactcccattatcc; size 199 bp.
CGR58; forward; tttttgccaattggttggat; reverse; gcctgggtgacagaggtaca; size 194 bp.
CGR67; forward; ttggtttaattttcagctgggta; reverse; ggaaagaaagagcactcaatgg; size 177 bp.
CGR69; forward; ttggcctttacaaacaaaagg; reverse; cttggtcaaggccagatag; size 185 bp.

DNA isolation, PCR and genetic analysis

Genomic DNA was isolated from peripheral blood as described previously (38). STR polymorphisms were amplified using 25 ng genomic DNA in 10 µl PCR reactions containing 1 × GeneAmp PCR Gold Buffer; 1.5 mM $MgCl_2$; 25 ng of fluorescent forward primer; 25 ng of unlabeled reverse primer and 0.4 units of AmpliTaq Gold DNA polymerase (Applied Biosystems). Initial denaturation was 10 min at 94°C followed by 32 cycles of 30 s denaturation at 94°C, annealing at 55°C and 90s extension at 72°C. PCR products were loaded on an ABI3100 automated sequencer (filterset D), data were analyzed using ABI GeneMapper 1.0 software. For haplotype analysis in family IT1, phase was assigned on the basis of the minimum number of recombination events.

Mutation analysis

Thyroid transcription factor 1 (TITF-1) has also been described as thyroid-specific enhancer-binding protein (T/EBP) and Nkx2.1. The genomic structure of TITF-1 was determined by aligning cDNA (XM_048680) and genomic sequences from BAC R-896J10. DNA was amplified using primers designed to flanking intronic sequence (at least 50 base intronic sequence) on both sides of an exon. The following primers were used:
Exon 1; forward; ggcagaagagaggcagacag; reverse; gggggagtaacagaggagga;size: 363 bp.
Exon 2; forward; agcgaggcttcgccttcc; reverse; ctctcgccgcacctccctg; size: 502 bp.
Exon 3_A; forward; gctaggctgcctgggtca; reverse; cgctgtcctgctgcagtt; size: 462 bp.
Exon 3_B; forward; gttccagaaccaccgctaca; reverse; gtttgccgtctttcaccag; size: 182 bp.
Exon 3_C; forward; caacaggctcagcagcagt; reverse; ggtggatggtggtctgtgt; size: 453 bp.

PCR reactions for exons 1, 2, 3_A and 3_C were performed in 50 µl containing 1 × GibcoBRL PCR buffer, 1.5 mM $MgCl_2$, 0.01% W-1, 250 µm dNTP, 0.4 µm forward primer, 0.4 µM reverse primer, 7% DMSO, 2.5 units Taq DNA polymerase (GibcoBRL) and 50 ng genomic DNA. Cycle conditions: 5 min at 94°C; 10 cycles of 30 s denaturation at 94°C, 30 s annealing at 65°C to 1°C per cycle (70°C to 1°C per cycle for exon 2) and 40s extension at 72°C; followed by 25 cycles of 30 s denaturation at 94°C, 30 s at 55°C (60°C for exon 2) and 40 s at 72°C; final extension 5 min at 72°C. Exon 3_B was amplified in 20 µl containing 1 × GCII buffer (TaKaRa) 400 µM dNTP, 1 µM forward primer, 1 µM reverse primer, 1 unit Taq DNA polymerase (TaKaRa LA) and 50 ng genomic DNA. Amplification was done using 1 min initial denaturation at 94°C; 35 cycles 30 s at 94°C, annealing 30 s at 55°C, 2 min extension at 72°C, final extension 5 min at 72°C. PCR products were purified using the Millipore Multiscreen PCR plates, and their approximate concentration was determined using Low DNA Mass Ladder (GibcoBRL). After direct sequencing of both strands using BigDye Terminator chemistry Version 4

(Applied Biosystems), Sephadex G50 (Amersham Biosciences) was used to purify the sequenced PCR products. Products were loaded on an ABI3100 automated sequencer and analysis was done with Sequence Navigator 1.0 for heterozygous base calls and sequence alignment.

Testing of the base changes/deletion in exon 3 in family US1 and UK1 in remaining family members (if available) and 200 control chromosomes from the general population was done using allele specific oligo hybridization (ASO). PCR products containing exon_3A for family US1 and exon_3C for family UK1 were blotted onto Hybond-N + (Amersham Biosciences). The blots were hybridized for 1 hour at 37°C in 5 × SSPE, 1% SDS and 0.05 mg/ml single-strand salmon sperm DNA with either the normal or mutated sequence primer. Filters were washed until a final stringency of 0.1 × SSC/0.1% SDS at 42°C.

The following primers were used for ASO hybridization: (G713T); W238L (US1); normal; agatctggttccag; mutated; aagatcttgttccag

(ΔG908) (UK1); normal; ggcgggtgccc; deleted; ggcggtgcccc

The mutation (C727A) R243S was confirmed in family NL1 and 200 control chromosomes by digestion of 10 µl PCR product in a 20 µl digestion reaction containing 1 × React1 and 10 units AluI (GibcoBRL). After digestion for 1 hour at 37°C, the products were run on a 2% agarose gel using 1 kb DNA Ladder (GibcoBRL) as a size standard. Normal individuals showed two fragments of 277 and 175 bp, respectively. Affected individuals in family NL1 showed three fragments of 277, 113 and 62 bases, respectively.

Amino acid alignment

Sequences were found by homology searches of the human TITF-1 protein to the non-redundant database using the BLAST algorithm. Aligning of the sequences was done using the program Vector NTI, which implemented the Clustal_W algorithm.

GenBank accession numbers

TITF-1 transcripts: HSU33749 for the short transcript and XM_048680 for the longer transcript. R-537P22: AL079304; R-552K16: AL121775; R-81F13: AL162464; R-964E11: AL079303; R-896J10: AL132857; R-356A6: AL137226; R-259K15: AL162511; R-116N18: AL133304; C-2577N12: AL133316.

CGR58: dbSTS_Id 104379, GenBank_Accn G73508; CGR69: dbSTS_Id 104378, GenBank_Accn G73507; CGR46: dbSTS_Id 104381, GenBank_Accn G73510; CGR67: dbSTS_Id 104380, GenBank_Accn G73509.

ACKNOWLEDGEMENTS

The authors wish to thank Drs M.F. Niermeijer and J.M. Hoogeboom for clinical support, Ms Lakshmi Srinidhi, Patrizia Rizzu and Bert Eussen for technical support, and Tom de Vries-Lentsch for artwork. This work was supported by the following grants: JanIvo Foundation to P.H. and NIH Grant NS16367 to M.E.M.

REFERENCES

1. Haerer, A.F., Currier, R.D. and Jackson, J.F. (1967) Hereditary nonprogressive chorea of early onset. N. Engl. J. Med., 276, 1220–1224.
2. Pincus, J.H. and Chutorian, A. (1967) Familial benign chorea with intention tremor: a clinical entity. J. Pediatr., 70, 724–729.
3. Hayden, M.R. Huntington's Chorea. Springer-Verlag, Berlin, 1981.
4. Harper, P.S. Huntington's Disease. W.B. Saunders London, 1991.
5. Harper, P.S. (1978) Benign hereditary chorea. Clinical and genetic aspects. Clin. Genet., 13, 85–95.
6. Haerer, A.F., Currier, R.D. and Jackson, J.F. (1966) Hereditary nonprogressive chorea of early onset. Neurology, 16, 307.
7. Bruyn, G.W. and Myrianthopoulos, N.C. (1986) Chronic juvenile hereditary chorea (benign hereditary chorea of early onset). In Bruyn, G.W., Vinken, P.J. and Klawans, H.L. (eds), Extrapyramidial Disorders. Elsevier Science, Amsterdam, Vol. 5, pp. 335–348.
8. Chun, R.W., Daly, R.F., Mansheim, B.J., Jr., Wolcott, G.J. (1973) Benign familial chorea with onset in childhood. JAMA, 225, 1603–1607.
9. MacMillan, J.C., Morrison, P.J., Nevin, N.C., Shaw, D.J., Harper, P.S., Quarrell, O.W. and Snell, R.G. (1993) Identification of an expanded CAG repeat in the Huntington's disease gene (IT15) in a family reported to have benign hereditary chorea. J. Med. Genet., 30, 1012–1013.
10. Klein, C., Wenning, G.K., Quinn, N.P. and Marsden, C.D. (1996) Ataxia without telangiectasia masquerading as benign hereditary chorea. Mov. Disord., 11, 217–220.
11. Zambrino, C.A., La Bounora, I., Lanzi, G. and Burgio, F.R. (1984) Corea benigna familiare: a proposito di due casi. G. Neuropsichiatr Eta Evol., 4, 81–87.
12. Schrag, A., Quinn, N.P., Bhatia, K.P. and Marsden, C.D. (2000) Benign hereditary chorea – entity or syndrome? Mov. Disord., 15, 280–288.
13. de Vries, B.B., Arts, W.F., Breedveld, G.J., Hoogeboom, J.J., Niermeijer M.F. and Heutink, P. (2000) Benign hereditary chorea of early onset maps to chromosome 14q. Am. J. Hum. Genet., 66, 136–142.
14. Fernandez, M., Raskind, W., Matsushita, M., Wolff, J., Lipe, H. and Bird, T. (2001) Hereditary benign chorea: clinical and genetic features of a distinct disease. Neurology, 57, 106–110.
15. Guazzi, S., Price, M., De Felice, M., Damante, G., Mattei, M.G. and Di Lauro, R. (1990) Thyroid nuclear factor 1 (TTF-1) contains a homeodomain and displays a novel DNA binding specificity. EMBO J., 9, 3631–3639.
16. Mizuno, K., Gonzalez, F.J. and Kimura, S. (1991) Thyroid-specific enhancer-binding protein (T/EBP): cDNA cloning, functional characterization, and structural identity with thyroid transcription factor TTF-1. Mol. Cell. Biol., 11, 4927–4933.
17. Ikeda, K., Clark, J.C., Shaw-White, J.R., Stahlman, M.T., Boutell, C.J. and Whitsett, J.A. (1995) Gene structure and expression of human thyroid transcription factor-1 in respiratory epithelial cells. J. Biol. Chem., 270, 8108–8114.
18. Harvey, R.P. (1996) NK-2 homeobox genes and heart development. Dev. Biol., 178, 203–216.
19. Kimura, S., Hara, Y., Pineau, T., Fernandez-Salguero, P., Fox, C.H., Ward, J.M. and Gonzalez, F.J. (1996) The T/ebp null mouse: thyroid-specific enhancer-binding protein is essential for the organogenesis of the thyroid, lung, ventral forebrain, and pituitary. Genes Dev., 10, 60–69.
20. Takuma, N., Sheng, H.Z., Furuta, Y., Ward, J.M., Sharma, K., Hogan, B.L., Pfaff, S.L., Westphal, H., Kimura, S. and Mahon, K.A. (1998) Formation of Rathke's pouch requires dual induction from the diencephalon. Development, 125, 4835–4840.
21. Sussel, L., Marin, O., Kimura, S. and Rubenstein, J.L. (1999) Loss of Nkx2.1 homeobox gene function results in a ventral to dorsal molecular respecification within the basal telencephalon: evidence for a transformation of the pallidum into the striatum. Development, 126, 3359–3370.
22. Pleasure, S.J., Anderson, S., Hevner, R., Bagri, A., Marin, O., Lowenstein, D.H. and Rubenstein, J.L. (2000) Cell migration from the ganglionic eminences is required for the development of hippocampal GABAergic interneurons. Neuron, 28, 727–740.
23. Mussell, G.M., Dure, L.S. and Percy, A.K. (1995) Benign familial chorea: clinical characterization of an Alabama pedigree. Neurology, 45, A184.
24. Guala, A., Nocita, G., Di Maria, E., Mandich, P., Provera, S., Cerruti Mainardi, P. and Pastore, G. (2001) Benign hereditary chorea: a rare cause of disability. Riv. Ital. Pediatr., 27(Suppl.), 150–152.

25. Hamdan, H., Liu, H., Li, C., Jones, C., Lee, M., deLemos, R., Minoo, P. (1998) Structure of the human Nkx2.1 gene. Biochim. Biophys. Acta, 1396, 336–348.
26. Li, C., Cai, J., Pan, Q., Minoo, P. (2000) Two functionally distinct forms of NKX2.1 protein are expressed in the pulmonary epithelium. Biochem. Biophys. Res. Commun., 270, 462–468.
27. Gruschus, J.M., Tsao, D.H., Wang, L.H., Nirenberg, M. and Ferretti, J.A. (1997) Interactions of the vnd/NK-2 homeodomain with DNA by nuclear magnetic resonance spectroscopy: basis of binding specificity. Biochemistry, 36, 5372–5380.
28. Damante, G., Fabbro, D., Pellizzari, L., Civitareale, D., Guazzi, S., Polycarpou-Schwartz, M., Cauci, S., Quadrifoglio, F., Formisano, S. and Di Lauro, R. (1994) Sequence-specific DNA recognition by the thyroid transcription factor-1 homeodomain. Nucleic Acids Res., 22, 3075–3083.
29. Albin, R.L., Young, A.B. and Penney, J.B. (1989) The functional anatomy of basal ganglia disorders. Trends Neurosci., 12, 366–375.
30. The Huntington's Disease Collaborative Research Group (1993) A novel gene containing a trinucleotide repeat that is expanded and unstable on Huntington's disease chromosomes. Cell, 72, 971–983.
31. Iwatani, N., Mabe, H., Devriendt, K., Kodama, M. and Miike, T. (2000) Deletion of NKX2.1 gene encoding thyroid transcription factor-1 in two siblings with hypothyroidism and respiratory failure. J. Pediatr., 137, 272–276.
32. Devriendt, K., Vanhole, C., Matthijs, G. and de Zegher, F. (1998) Deletion of thyroid transcription factor-1 gene in an infant with neonatal thyroid dysfunction and respiratory failure. N. Engl. J. Med., 338, 1317–1318.
33. Devriendt, K., Fryns, J.P. and Chen, C.P. (1998) Holoprosencephaly in deletions of proximal chromosome 14q. J. Med. Genet., 35, 612.
34. Kamnasaran, D., O'Brien, P.C., Schuffenhauer, S., Quarrell, O., Lupski, J.R., Grammatico, P., Ferguson-Smith, M.A. and Cox, D.W. (2001) Defining the breakpoints of proximal chromosome 14q rearrangements in nine patients using flow-sorted chromosomes. Am. J. Med. Genet., 102, 173–182.
35. Sutton, V.R. and Shaffer, L.G. (2000) Search for imprinted regions on chromosome 14: comparison of maternal and paternal UPD cases with cases of chromosome 14 deletion. Am. J. Med. Genet., 93, 381–387.
36. Nutting, P.A., Cole, B.R. and Schimke, R.N. (1969) Benign, recessively inherited choreo athetosis of early onset. J. Med. Genet., 6, 408–410.
37. Damasio, H., Antunes, L. and Damasio, A.R. (1977) Familial non-progressive involuntary movements of childhood. Ann. Neurol., 1, 602–603.
38. Miller, S.A., Dykes, D.D. and Polesky, H.F. (1988) A simple salting out procedure for extracting DNA from human nucleated cells. Nucleic Acids Res., 16, 1215.